Scientific Research Publishing

Open Journal of Geology, 2026, 16(4), 214-242
https://www.scirp.org/journal/ojg
ISSN Online: 2161-7589
ISSN Print: 2161-7570

Ordovician Sedimentary Processes and Related Driving Forces: Jordan, Arabian Plate

Werner Schneider[1], Elias Salameh[2]

[1](Retired) Institute of Geosciences, Braunschweig Technical University (TU Braunschweig), Braunschweig, Germany
[2]Department of Geology, University of Jordan, Amman, Jordan
Email: salameli@ju.edu.jo

How to cite this paper: Schneider, W. and Salameh, E. (2026) Ordovician Sedimentary Processes and Related Driving Forces: Jordan, Arabian Plate. *Open Journal of Geology*, **16**, 214-242.
https://doi.org/10.4236/ojg.2026.164012

Received: February 28, 2026
Accepted: April 21, 2026
Published: April 24, 2026

Abstract

The Ordovician-Lower Silurian siliciclastics deposited on the Jordanian Platform represent a transitional sedimentary system between their granitoid Gondwana source area and the Paleo-Tethys. While fluvial fining upward cycles (FUCs) of quartz arenite dominate braid plain deltas/upper shore face environments of the Lower Ordovician, arkosic tempestite and oxygen-deficient bituminous pelite/tuffite cycles cover upper/lower shore face environments of the Sandbian and Katian. The mineral deficit (feldspar, unstable heavy minerals) relates to acid sturz-rain events during volcanic degassing (SO_2, HCl, HF, NO_x) sourced in an Infracambrian/Cambrian Large Igneous Province (LIP) around S Sinai/Wadi Araba Rift-Zone. The change of sedimentary architectural elements/lithofacies types during the Upper Darriwilian took place after an L-chondrite of the Main Asteroid Belt (MAB) crossed the Earth's orbit (~470 Ma), which resulted in some small meteorite craters (*i.e.*, Lockne). Through the Sandbian and Katian, this insignificant impact series was accompanied by massive tephra production during worldwide explosive subduction-related volcanic arc magmatism. During the Upper Ordovician High Stand-System Tract (HST), the glass-bearing tephras were transformed under marine conditions into montmorillonite (K-bentonite), contributing to green tuffitic pelite interbedded with storm-generated arkosic clastics. Transtensional tectonics (pull-apart type) caused the main Ordovician-Silurian unconformity ("paleovalleys") in SE Jordan and Saudi Arabia. Their sedimentary fills expose arkosic FUCs originated by shallow-water turbidites during the Hirnantian. The intensive explosive volcanism generated almost continuously negative climate forcing ("cosmic winter") by tephra, aerosols, smog, and clouding that led to regional glaciation in the S Hemisphere. The abrupt $^{87}Sr/^{86}Sr$-ratio decrease accompanies, at the Sandbian base, the onset of magmatism, while $\delta^{13}C$ excursions follow a Transgressive System Tract (TST) and three T-maxima indicating increasing phytoplankton growth. The undulation—0% mirrors a

cyclicity of volcanic events, climate forcing, Eh, and pH conditions. The $\delta^{18}O$ rise shows a continuous CO_2 assimilation until its stop (~1200 ppm CO_2) and the following formation of black-shale facies.

Keywords

Sedimentary Processing, Volcanism, Comet/Impacting, Photosynthesis, Black-Shale Facies

1. Introduction

Matching tectonic quiescence [1]-[3], late Ordovician glaciation of the Gondwana hinterland [4]-[6], world-wide subduction-related explosive volcanism [7], impacts [8], and mass extinction [9] challenge sedimentary geologists/mineralogists.

May sequence-analytical patterns, cyclic lithofacies assemblages, and mineralogic data recorded from the Ordovician sedimentary systems of S Jordan verify interplaying causes and effects? The focus is on positive/negative climate forcing via tephra eruption [7], rift-degassing [1], and impact in connection with an L-chondrite breakup event in the main Asteroid Belt ~470 Ma ago [8]. The GSSP-chart (Stratigraphic Chart of Germany Compact), 2017 [10], was used for numerical age correlation.

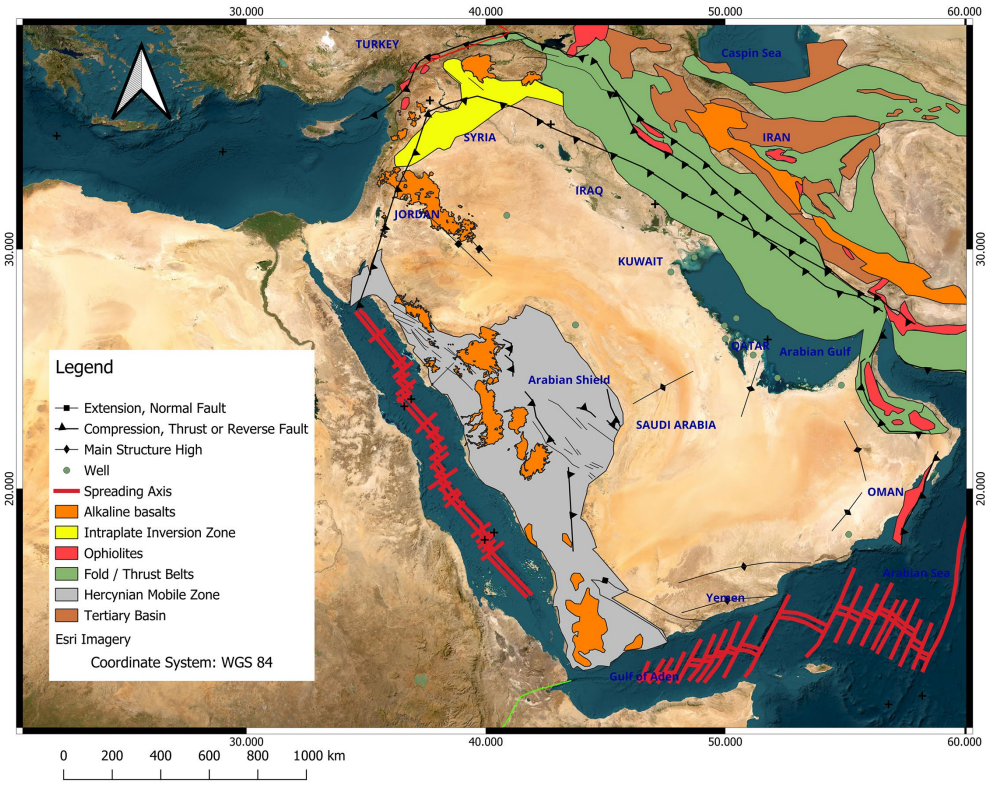

Figure 1. Major tectonic elements of the Arabian platform and adjacent areas. Jordan is located in the northwestern part and is confined by the wadi araba-dead sea fault zone [1]-[3].

A short paleogeographic excursion through the late Proterozoic (Ediacarian: 580 - 540 Ma) until the Cambrian/Ordovician b. (~485 Ma) introduces the subject:

After the fusion of the Arabian terranes with adjoining plates along the NE flank of Gondwana (~640 - 620 Ma), faulting (~620 - 580 Ma) and intracontinental Infracambrian extension (600 - 540 Ma: [1] [11]) were affected by the Wadi Araba rifting and the Najd-transform rift-system [1] [2] [11] (**Figure 1**).

As part of the Wadi Araba area, SW Jordan underwent the rift-related Abu Barqa granodiorite intrusion (610 ± 5 Ma), the Infracambrian Saramuj Conglomerate-event (~595 Ma), the Haiyala Volcano-clastic Series, and finally the explosive Aheimir/Feinan volcanics (550-541 Ma: [12]-[15]).

Both the Saramuj Conglomerate [13] and the arkosic L. Cambrian Saleb F. [16] represent synrift deposits; the latter covers the peneplained basement (Ediacarian/Cambrian b.: 541 Ma).

During a eustatic sea level rise [1] [2] [17], further rifting at the L./M. Cambrian b. (~510 Ma) led to the ingression of the Baltic Tethys along the later Jordan Valley-Rift [1]-[3]; **Figure 2(A)** and **Figure 2(B)**), where the Burj F. (510 Ma) exposes carbonate rocks and oxygen-deficient shales as Maximum Flooding Surface MFS [16]-[18].

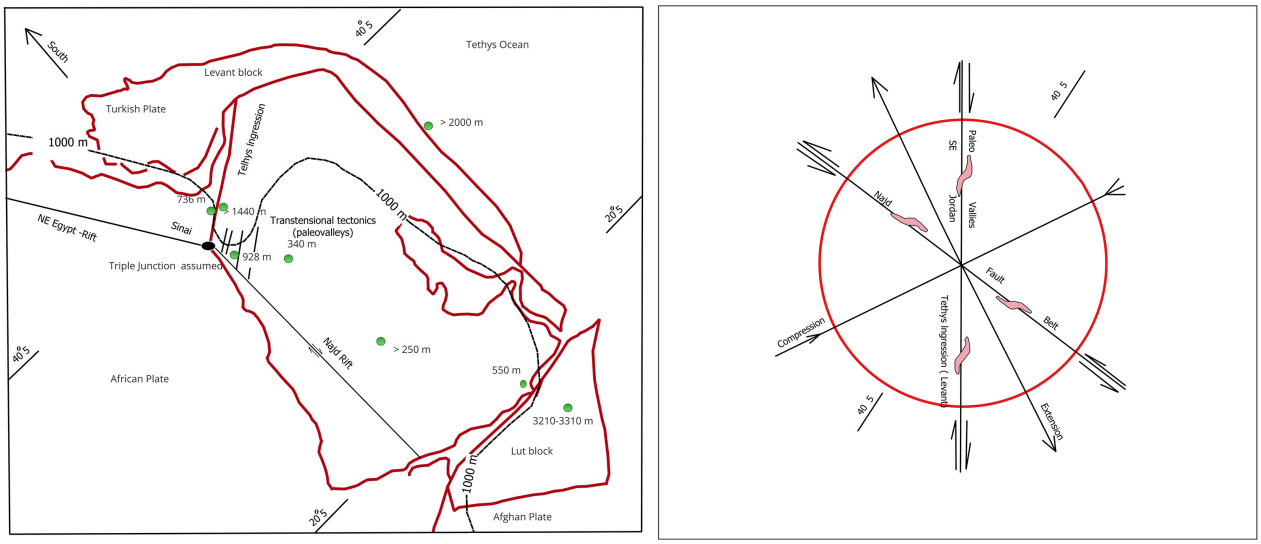

(A) (B)

Figure 2. (A) The 1000 m-isopach contour map indicates the Tethys ingression along a labile zone of tectonic weakness along the later Dead Sea-Jordan Valley Rift during the Early Paleozoic [1] [2]; (B) Deformation ellipsoid for the Early Paleozoic with regard to S Jordan and adjacent areas (Najd Fault Belt, transtensional tectonics/paleovalleys: Mudawwara area, Saudi Arabia).

The overlying Red Beds of the M/U. Cambrian Um Ishrin F. (~340 m), built up with quartz arenite-fining upward cycles (FUCs), rarely intercalated with thin pelite layers of marine incursions (Cruziana sp.), were deposited on unconfined braid plains [16] [18] and signal massive acidification by loss of feldspar and unstable heavy minerals [16] [18] [19].

2. Methodology

Methods applied: Sedimentology [20], mineralogy (thin sections, grain mounds), Clay mineralogy (XRD), geochemistry, pH, Eh, isotopes [21]. For the numerical ages of formations in Jordan references [3] [8] [10] were used.

3. Sediment-Geologic Inventory and Related Driving Forces

The following data are based on [16]-[31] (**Figures 3-6**; **Table 1**, **Table 2**).

Table 1. Architectural Elements (A) and lithofacies/sedimentary structures (B) completed for both fluvial and shallow marine environments [18] [20] [21].

(A)

Symbol	Element	Principal lithofacies assemblage
CH	Channel	Any combination
GB	Gravel bars and bedforms	Gm, Gp, Gt
SB	Sandy bedforms	St, Sp, Sh, Sl, Sr, Se, Ss
SG	Sediment gravity flow	Sm, Sh
DA	Downstream accretion macroform	St, Sp, Sh, Sl, Sr, Se, Ss
LA	Lateral accretion macroform	St, Sp, Sh, Sl, Se, Ss; minor Gm, Gt, Gp
LS	Laminated sand sheet	Sh, Sl; minor Sp, Sr
FF	Overbank fine sediments	Fl, Fm
MF	Mixed tidal flats	Sf, Sw, St, Sh, Fr, Fl
SF	Sandy tidal flat	St, Sf, Sw, Sl, Sr
SW	Sandwaves	St, Sp, Sh, Sl, Sr
TB	Tidal bar	St, Sr, Fr, Ss; Sf, Sw
T	Tempestite	Sh, Fl, Hcs, Scs, Sw
TCH	Tidal to subtidal channel	Sm, St, Sp, Sh

(B)

Facies code	Lithofacies	Sedimentary structures
Gmm	Matrix-supported, massive gravel	Weak grading
Gcm	Clast-supported massive gravel	Pseudoplastic debris flow
Gt	Gravel, stratified	Trough cross-beds
Gp	Gravel, stratified	Planar cross-beds
St	Sand, medium to very coarse, may be pebbly	Solitary or grouped trough cross-beds
Sp	Sand, medium to very coarse, may be pebbly	Solitary or grouped planar cross-beds
Sr	Sand, very fine to coarse	Ripple marks of all types
Sh	Sand, very fine to very coarse, may be pebbly	Horizontal lamination, parting lineation
Sm	Sand, fine to coarse	Massive or faint lamination
Ss	Sand, very fine to coarse, may be pebbly	Broad, shallow scours
Sl	Sand, very fine to coarse, may be pebbly	Low-angle (<15˚) cross-beds
Spo	Sand, fine to coarse	Overturned planar cross-beds

Continued

Sto	Sand, fine to coarse	Overturned trough cross-beds
Sf	Fine sand with mud	Flaser-rippled stratification
Sw	Fine sand with mud	Wavy-rippled stratification
Hcs	Fine sand and mud	Hummocky cross-stratification
Scs	Fine sand and mud	Swaley cross-stratification
Fr	Sand, silt, mud	Ripple- to climbing ripple cross-lamination
Fm	Sand, silt, mud	Massive
Fl	Sand, silt, mud	Fine lamination, very small ripples

Table 2. Faunal and Ichnofacies assemblages of the early Paleozoic of Jordan based on [18].

Era	**Cambrian**				**Ordovician**						**Silurian**	
Series	Lower		Middle	Upper	Lower		Upper				Lower	
Stage					Tremadoc	Arenig	Llanvirn	Llianc	Caradoc	Ashgill	Llandovery	
Formation **NW**	Salib Formation	Burj Formation	Umm Ishrin Formation	Disi Formation	Umm Sahm Formation		Hiswah Formation	Dubaydib Formation	Mudawwara Formation			Khushasha
Member **SE**		Abu Khushiba							Tubeiliyat. M	Ahmar Batra	Ratiya	
Graptolites							**__01**				**__**	**__02**
Brachiopods	**__**	**__B1__**							**__**	**__B2**		**__B3**
Acritarchs									**__**	**__**		
Cruziana Ichnofacies	**__**	**__C1__**	**__**	**__C2 __C3**	**__C4**		**__C5**	**__C6**	**__C7**			
Skolithos Ichnofacies	**__**	**__S1__**	**__**		**__S2**			**__S3 __S4**	**__S5**	**__**		
Scolicia		**__SC1**	**__SC2**									
Trilobites		**__T1**		**__T2**								

3.1. Upper Cambrian-Tremadocian-Floian, Disi F. (~320 m), (Figure 4(A), Figure 5(A))

During transtensional rifting between the Arabian Plate and the Levant Block [1], a pull-apart structure developed along the Wadi Araba when 650 m quartz arenitic FUCs (Um Ishrin, Disi F.) were deposited under high environmental acidification; thereby, subsidence and sedimentation rate seemed to be balanced on unconfined river-dominated braid plain deltas.

According to the high relevance of volatile degassing in LIPs and rift systems [32]-[35], and to magmatism that preceded in the realm of an assumed triple junction [1]: Sinai, Wadi Araba) up to the Ediacaran/Cambrian major unconformity (~541 Ma), we interpret the L./M. Cambrian hydrothermal Cu-mineralization at Timna/Feinan [16] [31], the loss of mineral constituents (feldspar, unstable heavy

minerals) from the arkosic L. Cambrian Saleb F. to the overlying quartz arenites, the absolute dominance of kaolinite/dickite [24]-[27], the lack of both carbonates and Fe^{3+} through the (white) Disi F., as effects caused by acids of volatiles like CO_2, CO, HC1, HF, and halo-methanes [32]-[35].

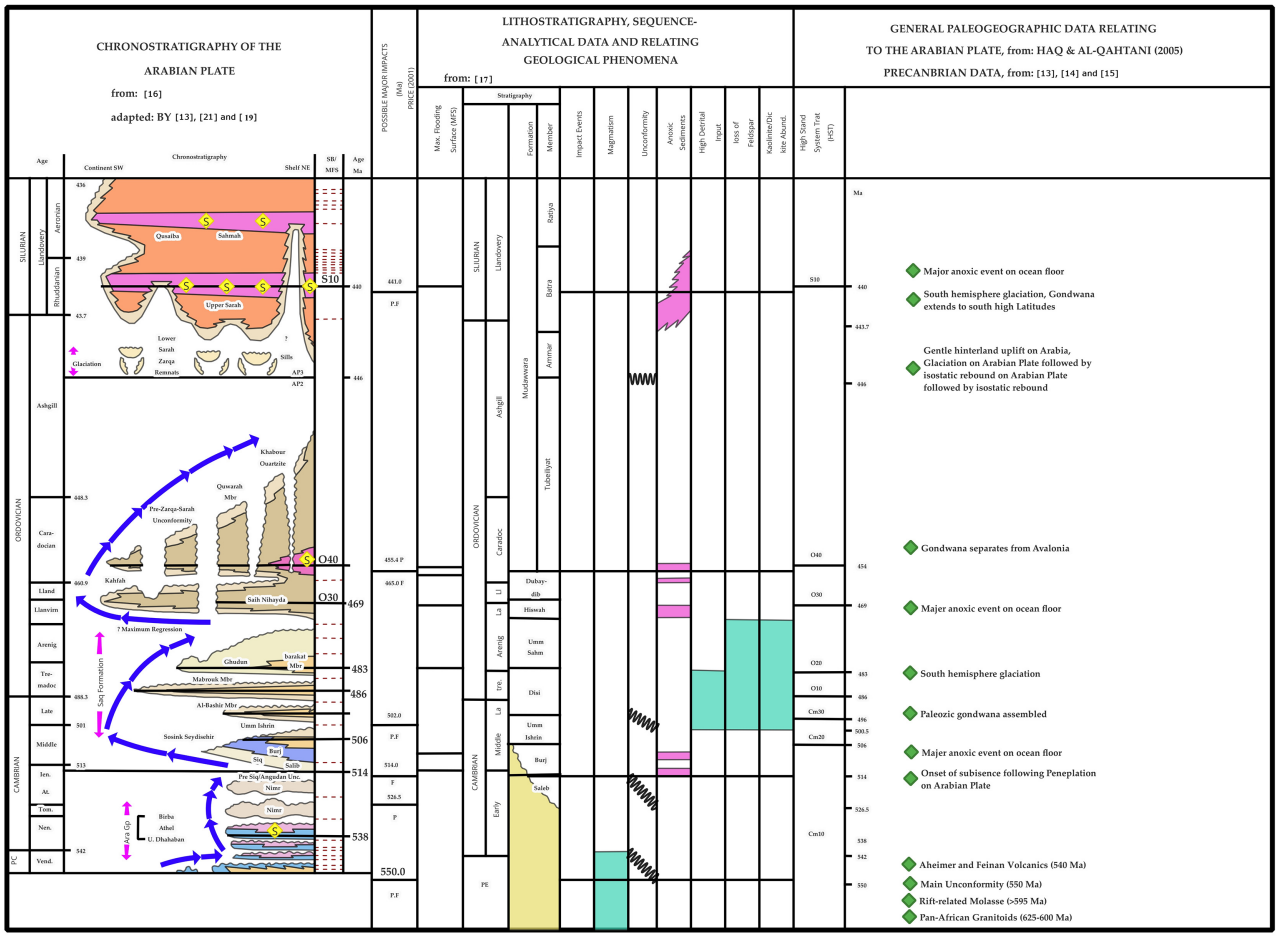

Figure 3. Chronostratigraphy, sequence-analytical data, and related geological patterns on the Early Paleozoic Jordanian Platform [19].

So, the sedimentologic/mineralogic change occurred after the Tethys invasion as a Transgressive System Tract (TST) and MFS during the global sea level rise [17].

The Um Ishrin/Disi F. b. appears unclear, yet is characterized by structureless mass flows (Gm, Sm, **Figure 4**), scattered manifold reworked quartzite pebbles (<12 km$^{\varnothing}$), chaotic hiatus/unconformity, change of rock color (red → white, Fe^{3+}-reduction), and sequence-analytical patterns, abruptly increasing sedimentary load to build large-dimensional, partly overturned FUCs beyond critical velocity.

The upper part of the Disi F. exhibits an increasing number of Cruziana-bearing pelite intercalations of early Tremadocian age [36], indicating a slowly rising sea level under continuous acidification.

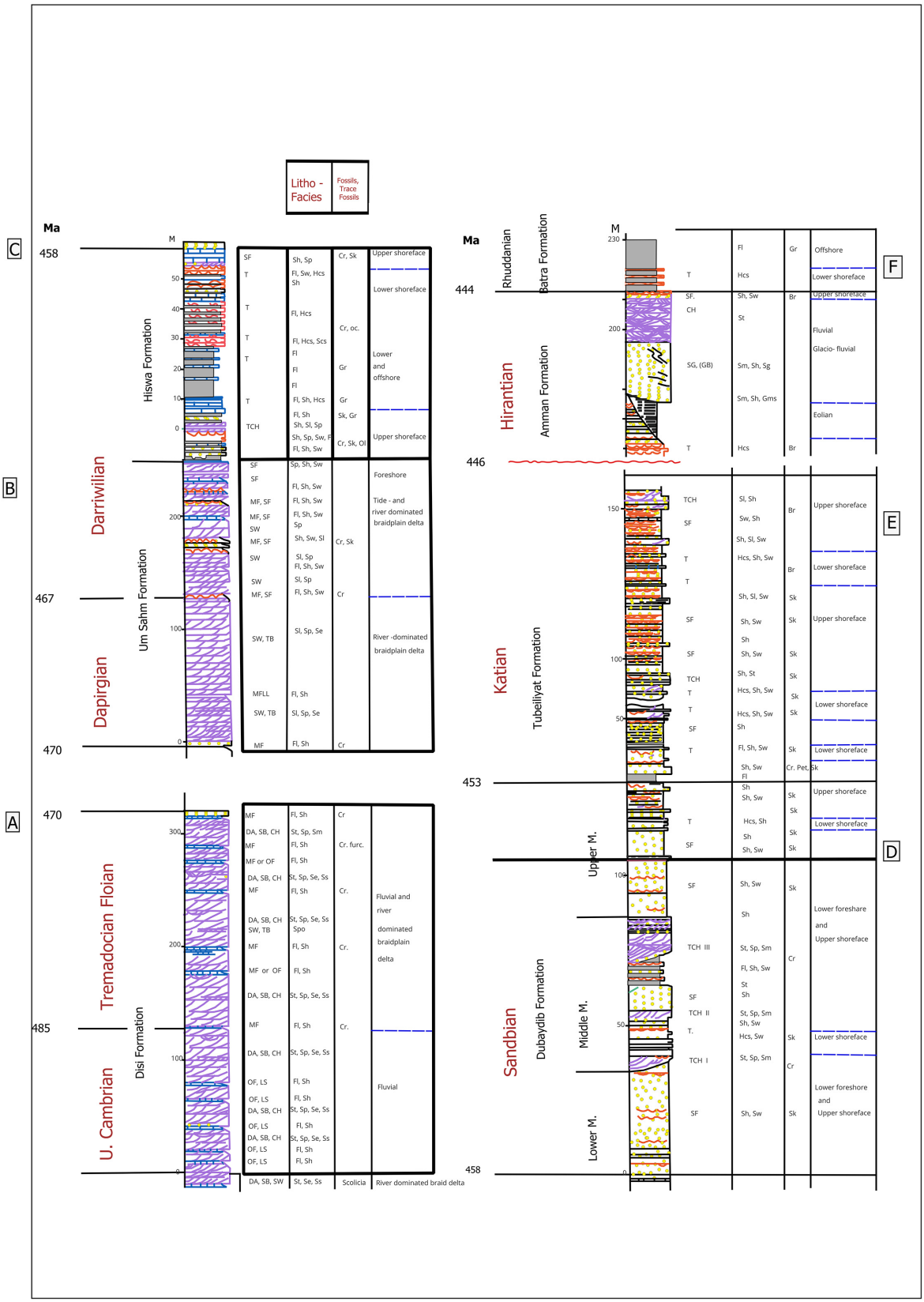

Figure 4. Architectural elements, lithofacies, fossils/ichnofacies, and depositional environments of the Ordovician, Jordan. A: Disi F. B: Um Sahm F., C: Hiswah F., D: Dubaydib F., E: Tubeiliyat F., F: Ammar F. [23]-[25].

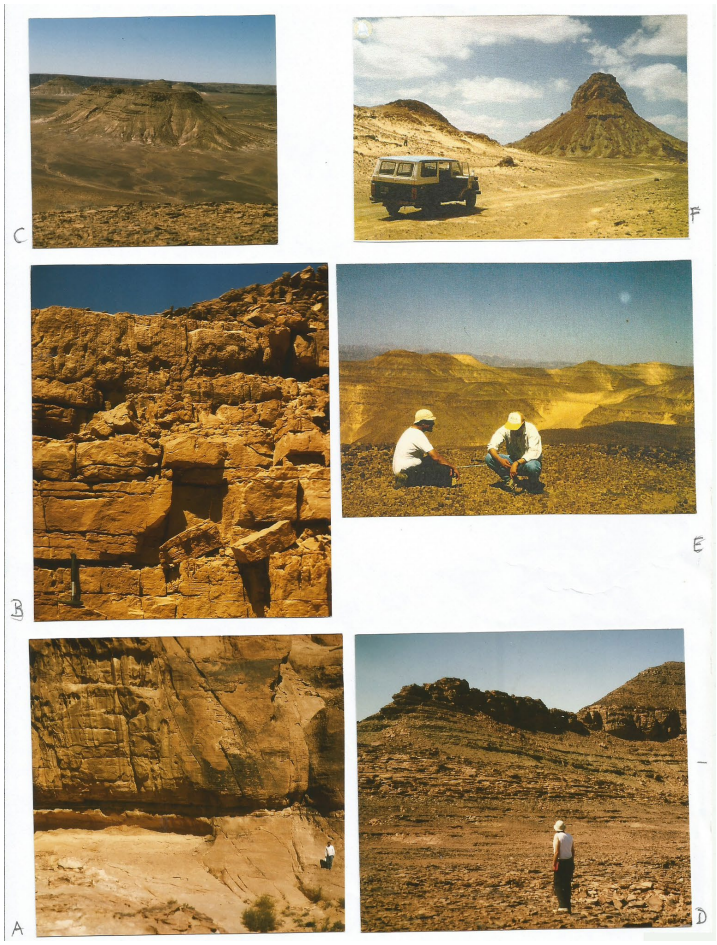

Figure 5. Field photographs of characteristic outcrops through the Ordovician, S-Jordanian desert. A: Disi F. (SG, DA), B: Um Salim F. (SB, Skolithos Sh), C: Hiswah F. (black-shale facies, graptolites), D: Dubaydib F. (CH), E: Tubeiliyat F. (T, Has, pelite/tuffite), F: Ammar F., Jebel Ammar (SG, MF, OSB-transition).

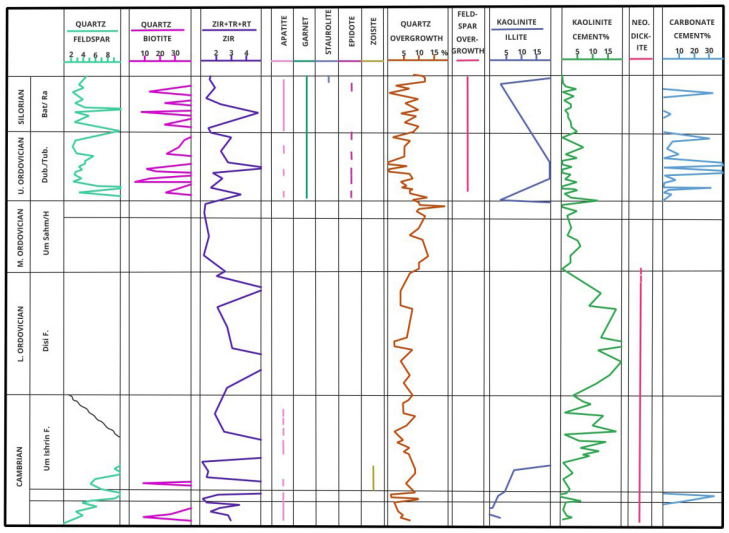

Figure 6. Sandstone mineralogy through the Cambrian and Lower Silurian S Jordan. Light/heavy m., clay m., and cement m [25] [27].

3.2. Dapingian to L. Darriwilian, Um Sahm F. (~260 m) (Figure 4(B), Figure 5(B))

Around the Floian/Dapingian b. (~470 Ma), a large L-chondrite (200 km$^{\varnothing}$) was disrupted in the Main Asteroid Belt (MAB), whose fragments crossed Earth's orbit for meteorite falls over the next several Ma (8: 470 - 462 Ma). Among them are the craters of Lockne (7.5 km$^{\varnothing}$), Mälingen (0.7 km$^{\varnothing}$), Kärdla, Granby, Tvären/Baltica, and those of Ames, Calvin, Brent, Slate Island, Pilot, Couture/Laurentia, as well as the meteorite falls of Kinnekulle and Brundflo/Baltica, within the timespan 470 - 430 Ma [8].

A velocity change of Moon recession from 10.73 to 12.86 km/Ma was recorded for the same time interval [35], while intensive explosive subduction-related tephra volcanism commenced on a global scale [7] (**Figure 7(A)** and **Figure 7(B)**).

Contemporaneously, carbonate- and fossil-free quartz arenite FUCs of the Um Sahm F. were deposited on distal unconfined braid plain deltas and intertidal environments. Around 467 Ma, short marine incursions documented by Cruziana-bearing pelites indicate a slow sea level rise. However, high maturity, low quartz syntaxial overgrowth, and kaolinite cement underline a continuation of seawater acidification.

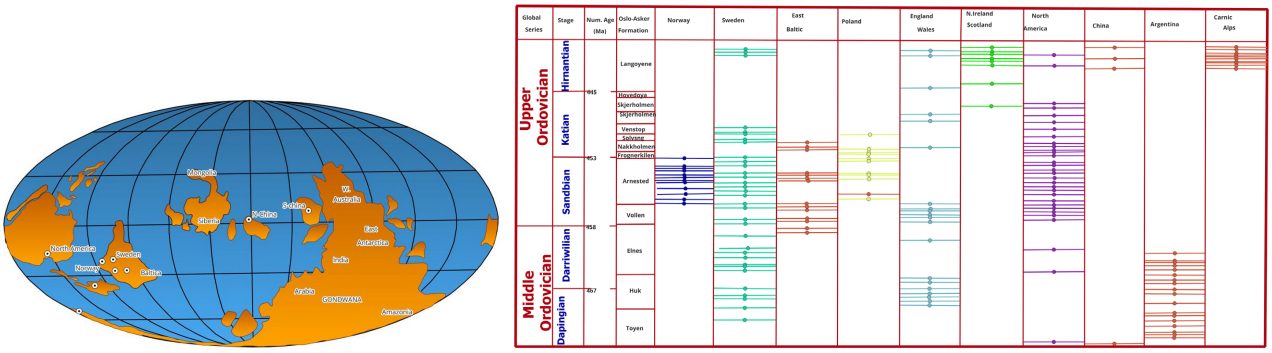

(A) (B)

Figure 7. Paleogeographic distribution of K-bentonite occurrences around 450 Ma (A) and global distribution of Middle and Upper Ordovician K-bentonites (B) [7].

From there, through the U. Um Sahm F., the first tephra deposits [7] (**Figure 7**), transformed to K-bentonite, became relevant as a tuffite component.

Because of their small size, both meteorite finds and impact craters may play a subordinate role in the following "tephra/K-bentonite concert" without verification of shocked quartz (PDSs) and micro-tektites.

3.3. Upper Darriwilian, Hiswah F., (~60 m), (Figure 4(C), Figure 5(C))

The oxygen-deficient sequence represents a TST towards an upper shore-face environment exposing Cruziana-, Skolithos-, and Diplocraterion ichnofacies, finally culminating in an MFS connected with a eustatic sea level rise [17] by deposition

of graptolite-bearing black-shale facies of lower shore-face and offshore, still interbedded with quartz arenite intercalations as tempestites (Hcs).

Atop the Hiswah F., the acidification of seawater ceased with increasing frequency of the first K-bentonite layers in Sweden and England [7], impacting Baltica [8].

3.4. Sandbian to L. Katian, Dubaydib F., (130 m), (Figure 4(D), Figure 5(D))

The Darriwilian/Sandbian b. (~458 Ma) coincides with the Lockne and Malungen impact [8]. During the following High Stand System Tract (HST), the arkosic siliciclastics exhibit lower maturity (feldspar, unstable heavy minerals) compared to the underlying formations, a decrease in quartz-syntaxial overgrowth, and clay-mineralogical dominance of illite, chlorite, mixed layer minerals, montmorillonite, and carbonate cement [25] [27] (**Figure 6**), indicating a pH increase in seawater. Skolithos- and Cruziana-ichnofacies-bearing siliciclastics were deposited in shore face environments [18] [19] [22] [26].

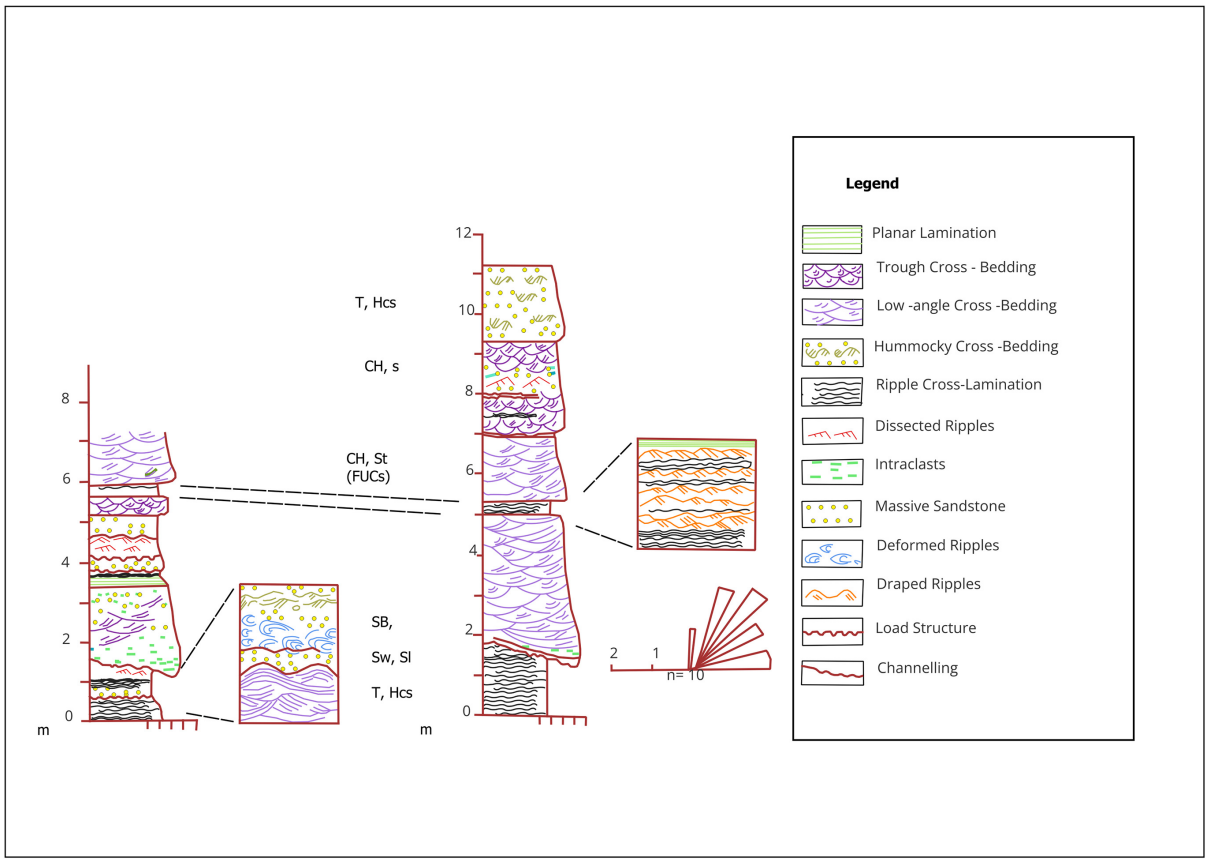

Figure 8. Lithofacies sequence in a transtensionally originated channel (strike-slip tectonics) in the middle Member of the Dubaydib F., SE Jordan [26].

However, the middle member of the Dubaydib F. (**Figure 4**) displays storm- and sturz rain-dominated mass flows exposing amalgamated FUCs (Sm, St, Sp) as

fills in three prominent submarine channels (TCH I - III) containing intraformational lag deposits, boulders up to 2 $m^{\varnothing}$, and overturned cross-bedding (DA). The channels have a width of 8 - 80 m, a depth of 2.2 - 12 m, and a consistent unidirectional fore-set azimuth towards NE, eroding the underlying pelite by proximal turbidite-like processing [26] (**Figure 8**).

With regard to the formerly active Najd- and Wadi Araba-rifting [1], we interpret the channel formation as reactivated sinistral transform faults/transtensional strike-slip valleys with water depths of several tens of meters (**Figure 2(B)**). The channel deposits are composed of reworked siliciclastics from the southward-located river-dominated braid plain deltas. The synsedimentary tectonics coincides with a high frequency of K-bentonite occurrences encountered in Norway, Sweden, E Baltica, Poland, and N America around 455 Ma (**Figure 7(A)**, **Figure 7(B)**), which represent associated material in the grey-green tuffitic pelites.

The high-energy activities ceased during the upper member of the Dubaydib F. by the deposition of ichnofacies-bearing shore-face tuffitic pelites and tempestites (Hes) [18] [22] [26]; thus, the latter display coarsening-upward cycles (CUCs) in contrast to the FUCs of the channel deposits.

3.5. Katian, Tubeiliyat F. (105 m), (Figure 4(E), Figure 5(E))

The Dubaydib/Tubeiliyat transition exhibits a prominent varicolored shaly marker up to 15 m thick [18] [22] [26] (**Figure 9(A)**). XRD analysis of several green pelite layers verifies a significant amount of montmorillonite, regular/irregular montmorillonite-bearing mixed layer minerals, and chlorite [22] [25] (**Figure 9(B)**), which meets the eruptive event series of K-bentonite (see above) and the impact events of Brent, Slate Island, and Calyn/I.aurentia [8] (453 - 450 Ma).

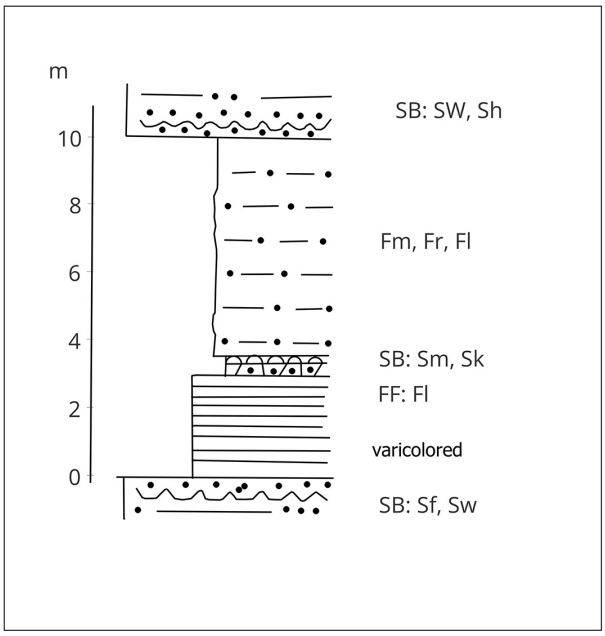

(A)

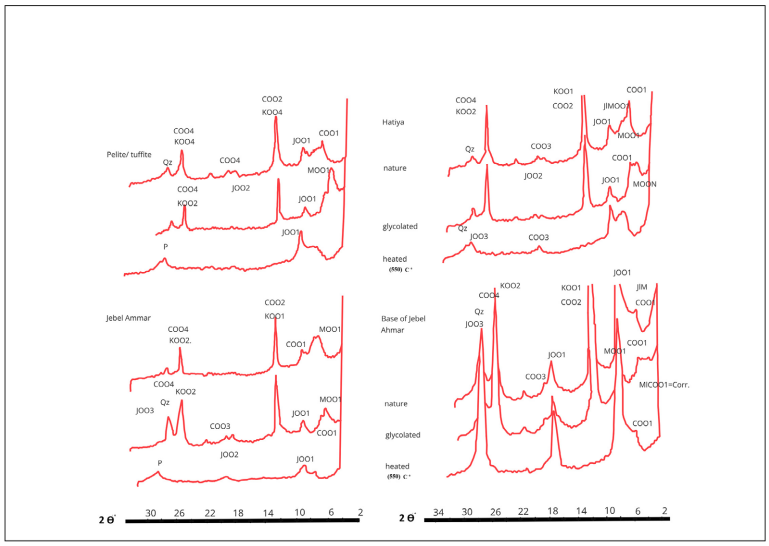

(B)

(C)

Figure 9. Tubeiliyat F.: Tempestite-pelite/tuffite cycles, Mudawwara area [6] [26] [28] (A): Dubaydib/Tubeiliyat "boundary clay"; lithofacies [26]. (B): Clay mineralogy of pelite/tuffite beds; XRD analysis, G 2 pm basal reflections 001, 002, 003, 004, [6]. a: pelite/tuffite, Mudawwara area, b: Jebel Ammar, c: Hatiya, d: mudstone clasts at the bottom of Jebel Ammar [6]. Q quartz, K kaolinite 001, 002; I illite 001, 002, 003; C chlorite 001, 002, 003, 004; M montmorillonite 001, 002; I/M irregular illite/montmorillonite mixed layer 001; M/C regular montmorillonite/chlorite mixed layer = corrensite. (C): Tempestite, hummocky cross-stratification (Hcs), Tubeiliyat T., Mudawwra area.

The Tubeiliyat F. consists of cyclically interbedded green pelite units and storm-generated siliciclastic tempestites (T, Hcs) deposited in shore-face environments (**Figure 9(C)**), where lingulacean brachiopods appear in the upper part [26].

In contrast to the U. Cambrian-L. Ordovician time span (quartz arenite), the siliciclastics of the M.-U. Ordovician arkosic/subarkosic sandstones dominate the Ordovician, where feldspar, biotite, and unstable heavy minerals are preserved, indicating shorter transport, ceasing acidification, and rare carbonate cement [25] [27].

Concerning lithofacies and architectural elements, coincidence with the Dubaydib F. is proposed to coalesce both into one Formation for correlation with the subsurface Tarifa F. [26] [29] [30].

There may be a challenge to correlate the pelite/Hcs-cycles with the lithostratigraphy of the Oslo region [7].

The top of the Tubeiliyat F. is marked by a major erosional unconformity ("paleovalleys") in S Jordan and Saudi Arabia [5] [6] [9] [22] [26] [28]-[30].

3.6. Hirnantian, Ammar F., (0 - 300 m), (Figure 5(F), Figure 6(F))

The Ammar F. crops out in NW Mudawwara, SE Jordan, and in Saudi Arabia [6] [18] [22] [26] [28] [29]; it is also encountered by drilling [30]. The arkosic/subarkosic suite is restricted to and preserved in several submarine canyons ("paleovalleys"), interpreted as fluvial-glaciofluvial deposits during the deglaciation of the Gondwana hinterland, located ~100 km from the ice sheet that covered wide areas of N Africa and Saudi Arabia (**Figure 10(A)**, **Figure 10(B)**).

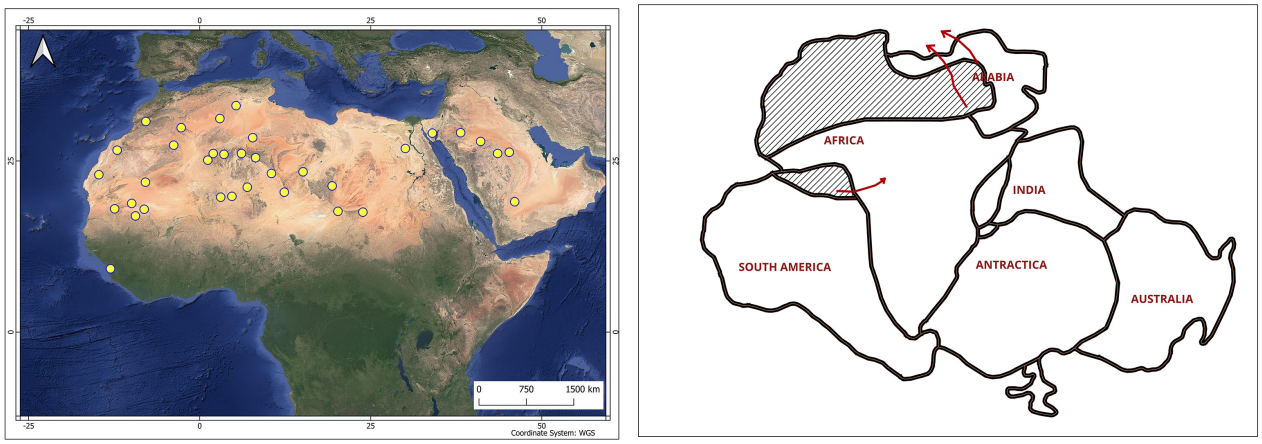

(A) (B)

Figure 10. Occurrence of glaciofluvial deposits (Hirnantian) in N Africa and the Near East (A). Glacial areas in N Africa, the Near East, and northeastern S America (B), [4]-[6].

The submarine canyons of S Jordan expose NNW-resp. NNE-striking, with a width of 0 - 4 km and a length of up to ~70 km (**Figure 11**), and obviously follow reactivated transform faults of the early Wadi Araba rift [1]. We interpret them as transtensional strike-slip structures (pull-apart type) scoured by synchronous fluvial-glaciofluvial processes; this is well verified by steep flanks, slumping, and reworked boulders of the Tubeiliyat F. [6] [18] [22] [28]. Mass flows and amalgamated FUCs build up the fill of the canyons (**Figure 12**). Lag deposits consist of Cambrian/Ordovician faceted and striated quartzite pebbles and basement rocks (*i.e.* biotite-granite).

Some 50 km NW of Mudawwara, at the eastern rim of Wadi Hiswah, Jebel Ahmar exposes a 70 m thick sequence built up with major FUCs [28] [29]; (**Figure 12**); each cycle has an erosional base, lag remnants, and structure-parallel flow

direction.

As meanwhile experienced from other Phanerozoic siliciclastic formations of the Jordanian Platform [16] [18] [19] [24], the FUCs represent sturz rain events caused by atmospheric hazards.

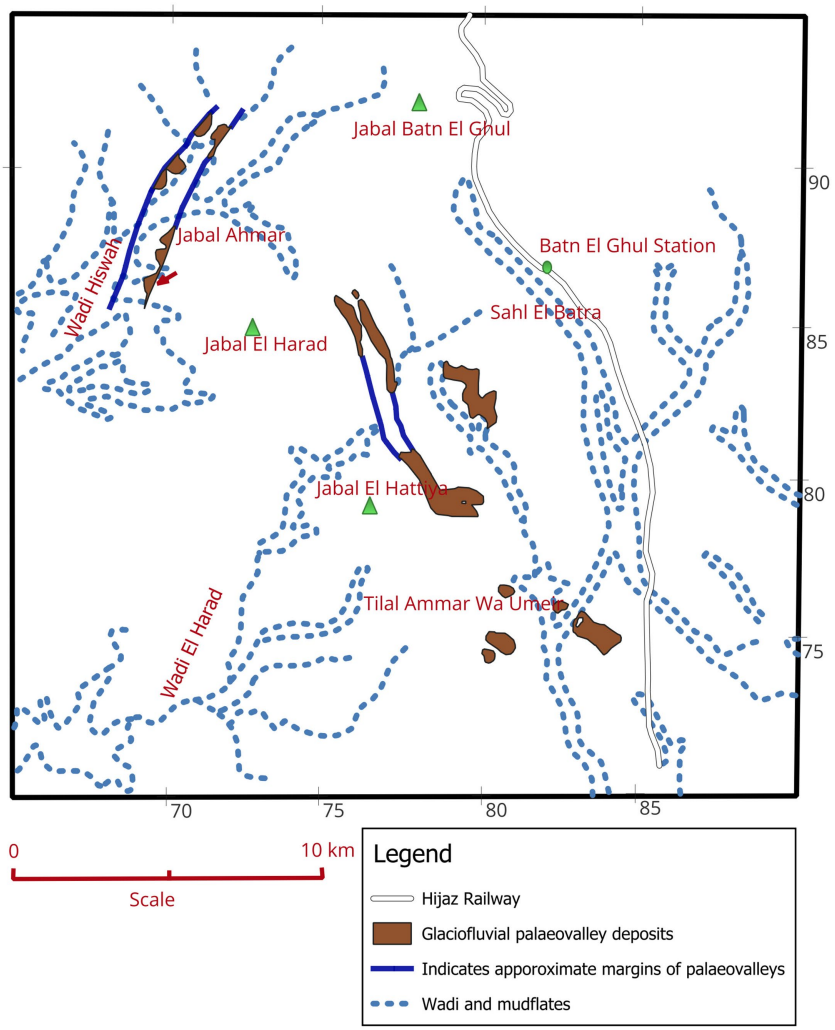

Figure 11. Occurrence of Hirnantian glaciofluvial deposits preserved in transtensionally. Originated paleocanyons (graben structures) in the Mudawwara area, S Jordan. Type locality: Jebel Ammar [6] [18] [22] [27] [28].

The base of the Jebel Ahmar section contains large angular boulders of green pelite (**Figure 9(A)**) with high amounts of montmorillonite and its mixed-layer minerals, reworked from the Tubeiliyat F. or from the underlying boundary clay [22] indicated by X in **Figure 4(E)**, already mentioned above with regard to the coincidence with massive tephra production during the U. Sandbian (~455 Ma) in the Northern Hemisphere [7].

As type-localities, both Jebels Ammar and Umeir (**Figure 13**), situated between Mudawwara and Jebel Ahmar, expose the uppermost part of the Ammar F. and its transition to the Silurian Batra F. inside the graben-like canyon [18] [22] (**Fig-**

ures 13(A)-(E), Figures 14(A)-(C)); lag-deposits and a mass flow (Sm, Sh, Sg) scour several-meter-thick structureless, well-sorted fines (Fm) of silt-fraction (2-63 μm) (paleoloess), deposited in an eolian or subaquatic environment (Figure 13(D)). The Hirnantian/Silurian b./transition crops out in the type area Batu en Ghul, Mudawwara (Jebels Ammar, Umeir), shallow water black shale facies coeval with transtensional tectonics; high $\delta^{13}C$ = + 7‰ possibly "methane-eruption", most important hydro-carbon source interval on the Arabian Plate.

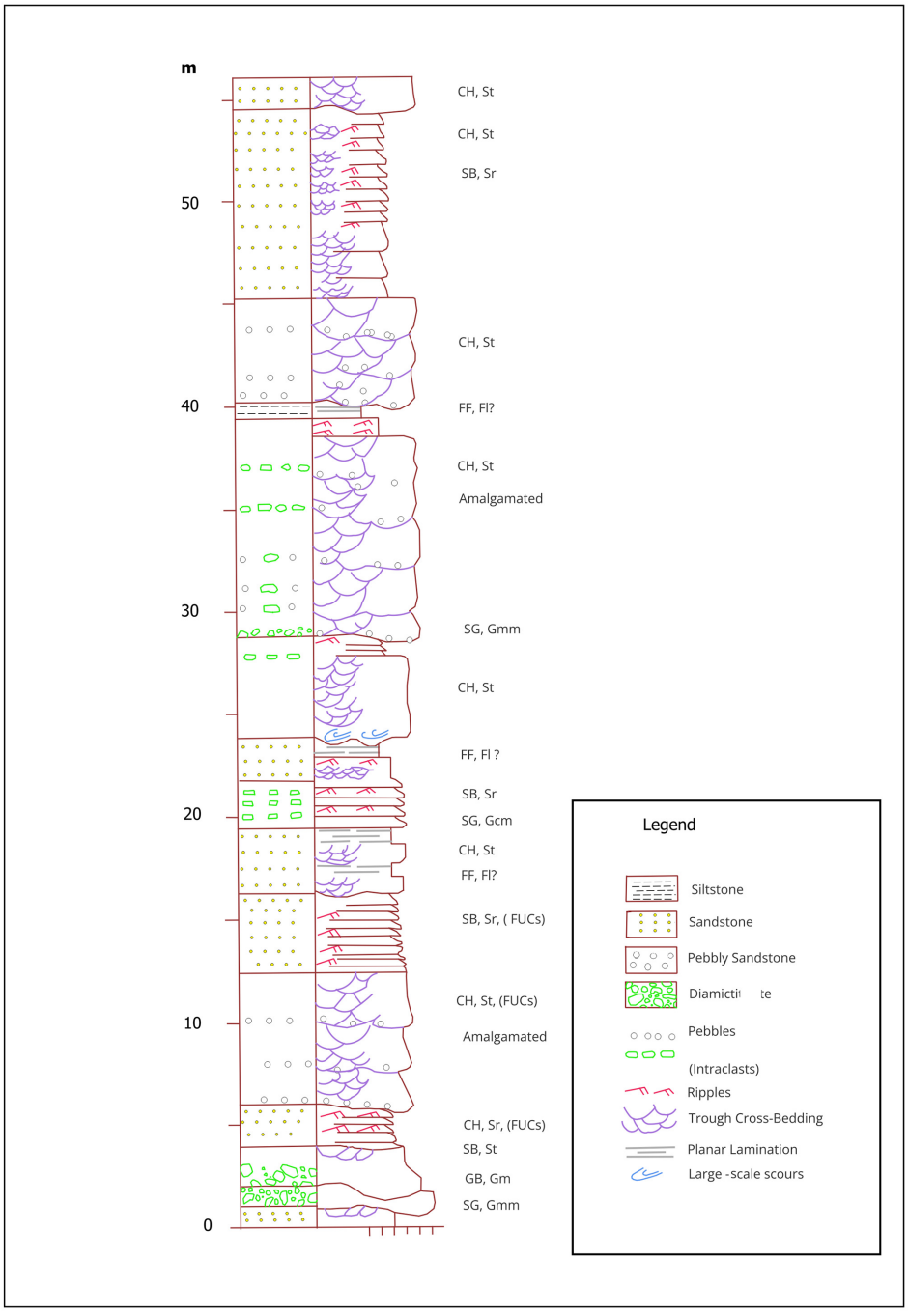

Figure 12. Lithofacies log of the paleocanyon fill at Jebel Ahmar [27].

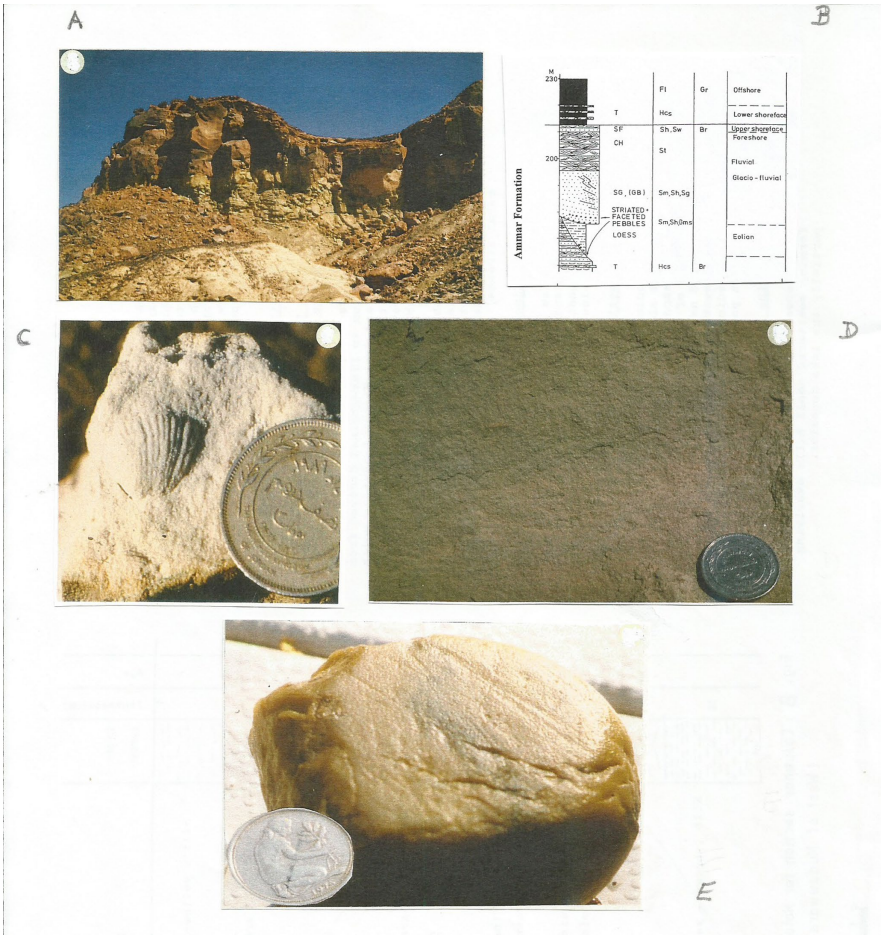

Figure 13. The upper part of the Hirnantian at Jebels Umeir and Ammar, located north of Mudawwara. A: Top of Jebel Umeir; subaquatically deposited paleoloess overlain with lag deposits, fluvial, and shallow marine siliciclastics (see Figures 13(B)-(E)); B: Lithofacies of the Hirnantian/Rhudannian b. (OSB); C: Brachiopods Mentacella sp. [36]: embedded in coarse-grained arkosic shallow marine sandstone; D: Well-sorted, structureless siltstone, paleoloess submarine deposited. E: Faceted and striated quartzite pebble as a component of the lag deposits (Figure 13(A)).

The overlying siliciclastics are of current origin (St), changing to fore-shore and upper shore-face environment (SF); the latter bear brachiopod imprints, possibly Mentacella sp.? [36] (**Figure 13(C)**). The section develops to tempestites (Hcs) and finally to graptolite-bearing black-shale facies (**Figures 14(A)-(C)**); Hcs indicates a water depth of 5 - 30 m [37].

The upper part of the Hirnantian exposes a series of tephra eruptions originating in the Carnian Alps, Sweden, N Ireland/Scotland, N America, and China (**Figure 7(A)**, **Figure 7(B)**), which are the main co-players through the Ordovician-Silurian transition.

Outside the marine canyons located in the Mudawwara area, the 60 m thick Batra F. is mainly composed of interbedded grey-green pelite and fine-grained siliciclastics of shore-face environments without any visible unconformity or prominent black-shale facies [25] (**Figure 14(A)**). The overlying 80 m thick Ratiya

F. exposes shore-face arkosic siliciclastics, intercalated with a few pelite layers that are rarely carbonate-cemented, overlain by a few tempestites. Obviously caused by the uplifting Gondwana hinterland and a consequent sea level drop [3], the Batra black-shale facies diachronously migrated northward [28] [29]. Thus, in contrast to the Hiswah F. and the marine canyons of the Hirnantian, the oxygen-deficient facies developed outside the canyons in shallow marine hollows or is even missing [28] [29], without any indication for TST, MFS, or SB (Sequence Boundary).

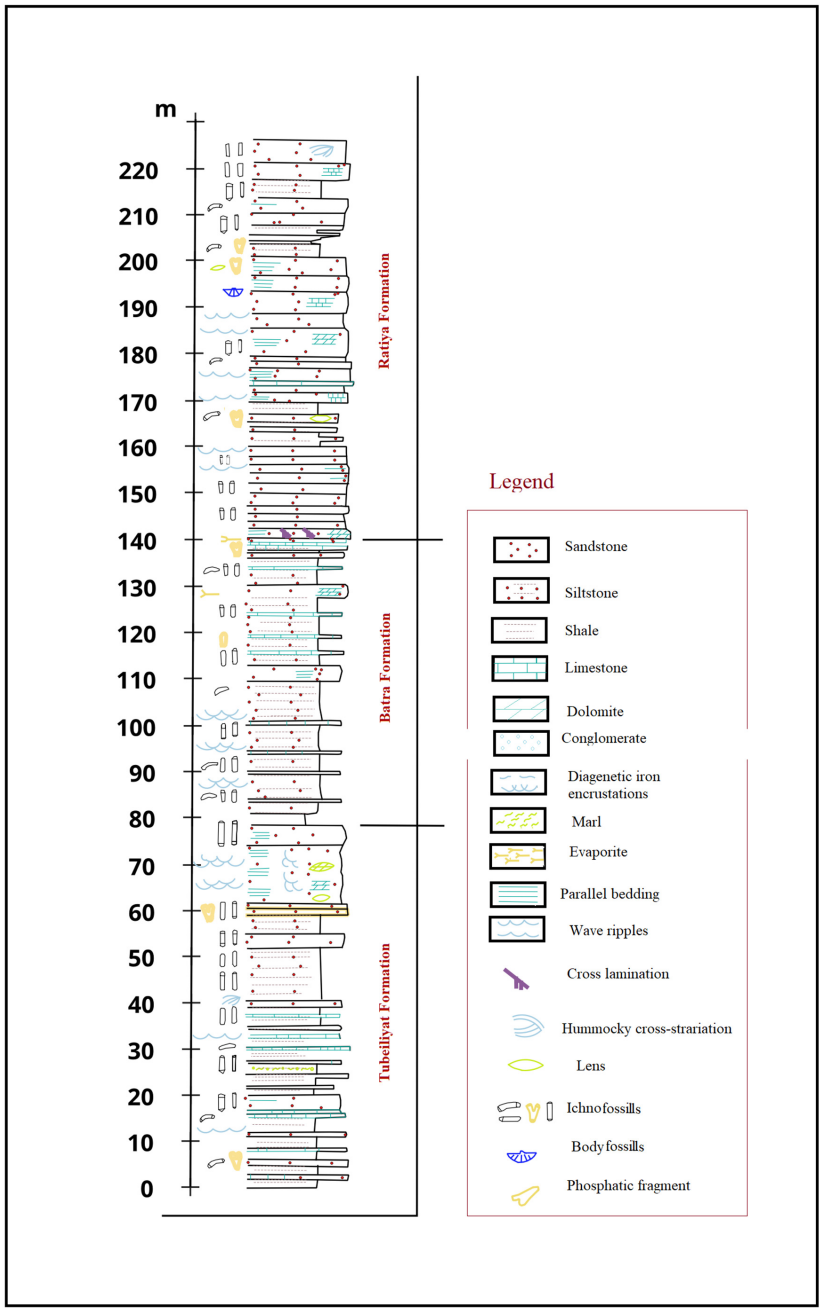

(a)

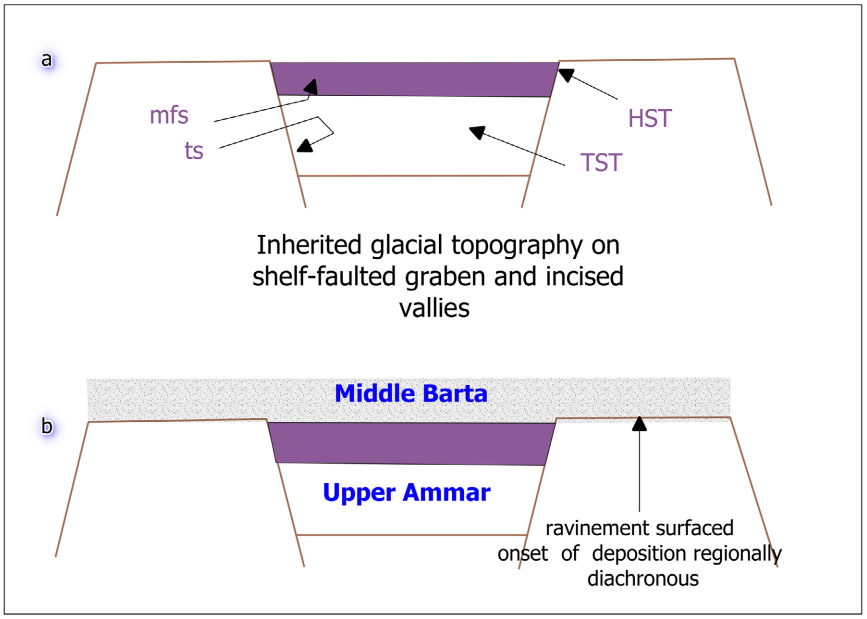

(b)

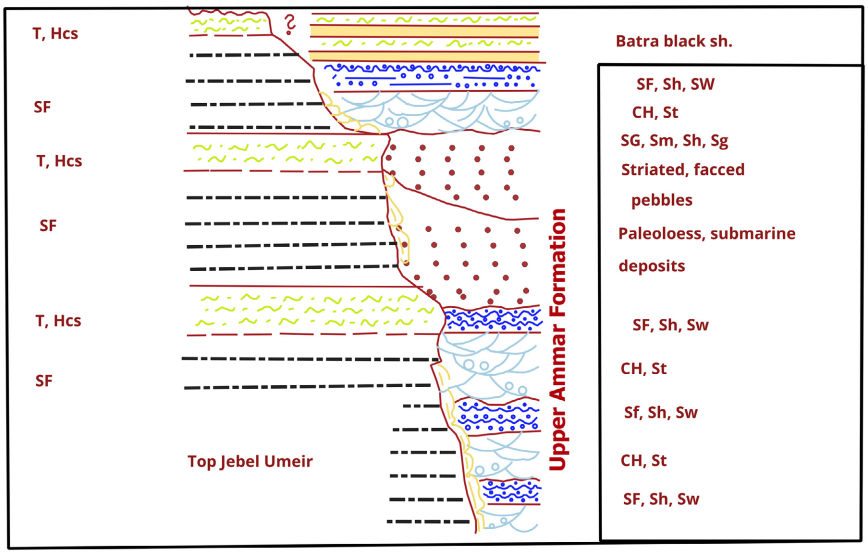

(c)

Figure 14. Hirnantian/Rhuddanian transitional zone (OSB.) in the Mudawwara area, SE Jordan [25] [26] [28]. a: Lithostratigraphic sequence of the Upper Tubeiliyat-Hirnantian Rhuddanian F. [25] [26]; b: Uppermost part of the paleocanyon (graben)-fill at type loc. Jebel Ammar [18] [29]. Note the first occurrence of black-shale facies in the Upper Hirnantian, directed by transtensional tectonics, and its absence outside the paleocanyon.

Inside the "canyons" (pull-apart structures), the black-shale facies started during the late Hirnantian syntectonically and immediately after the deposition of fore-shore/shore-face siliciclastics under trans-tensional tectonics (**Figure 14(C)**), followed above an unconformity by the sequence: paleoloess, gravity mass flow, fore-shore/shore-face black-shale facies. The latter extends around the Gondwana margin [4]-[6].

4. Driving Forces—Dynamic Networking—Sedimentary Deposits (Figure 15) Paleogeographic Basics

Except for the Hirnantian, the L./M. Ordovician of S Jordan underwent tectonic quiescence during gentle sea level rise (LST → TST → MFS → HST) (LST = Low Stand Track). However, plate motion was identified since 455 Ma concerning Hawai and Fennoscandia [35] (**Figure 16(A)**, **Figure 16(B)**), overall with massive cyclic Sandbian tephra production and transtensional tectonics after the Lockne impact [7] [8]. The loss of unstable minerals in the distal quartz arenites FUCs was caused during the Tremadocian to Darwillian under tropical climate and atmospheric hazards (sturz rain) by environmental acidification sourced from degassing of the Wadi Araba rift-system [1] [11] [13] [14] [24]. The Sandbian plays a transitional role (MFS) after the MAB-event (~470 Ma), followed by minor impacting and the change in the Moon recession rate [35].

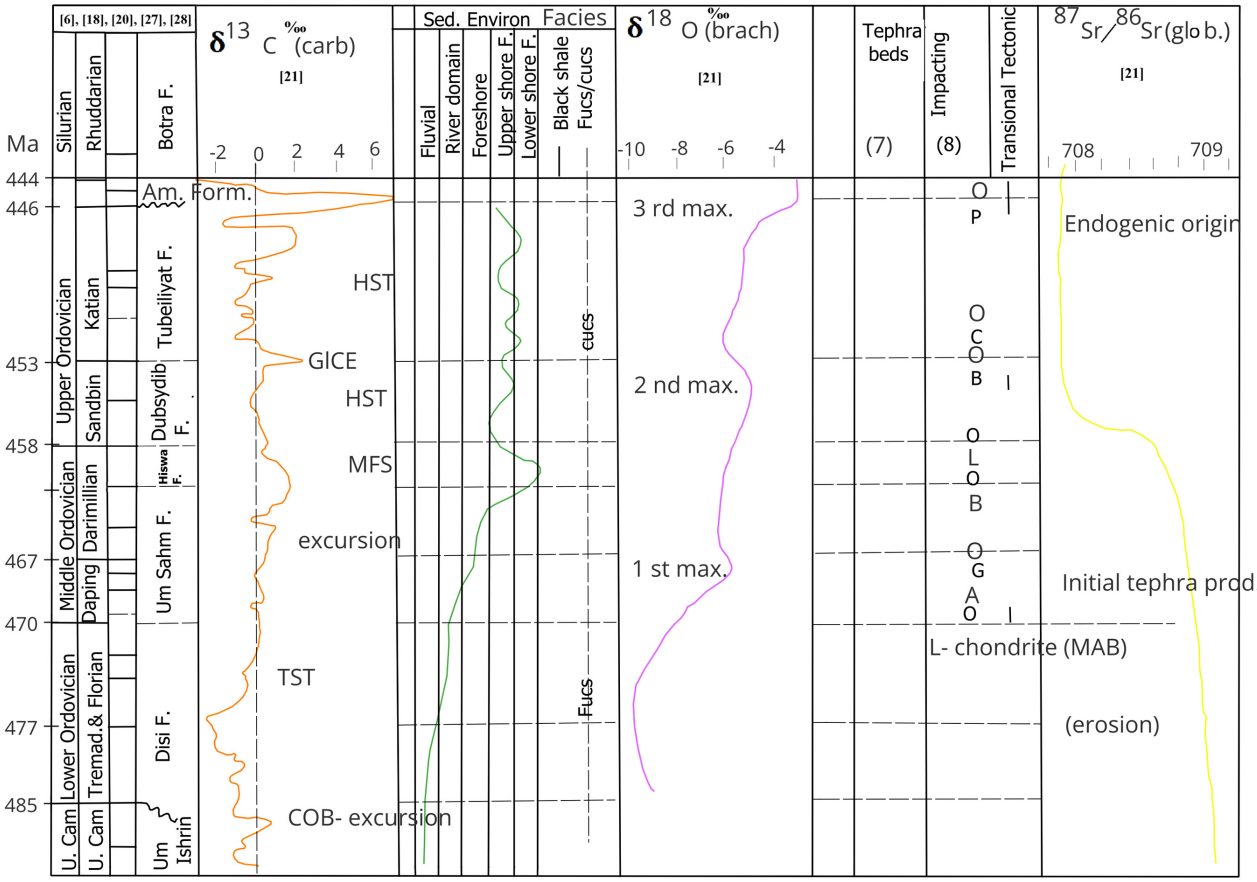

Figure 15. Chart of the sedimentary inventory (lithofacies, sequence analysis, environment), drivers through the Ordovician: volcanism, impacting, transtensional tectonics, isotope excursions ($\delta^{13}C$, $\delta^{18}O$, $\delta^{87}Sr/^{86}Sr$), and climate forcing.

After 450 Ma, the Sandbian to Katian time-span exposes storm-generated arkosic tempestite/pelite-tuffite cycles (−20) during inner Gondwana glaciation, proximal glacio-fluvial sediment transport, decreasing temperature, and physical weathering in undulating shore-face environments.

The black-shale facies of the Hirnantian-Silurian transition demands a significant CH_4-event through the final filling of the trans-tensional graben structures.

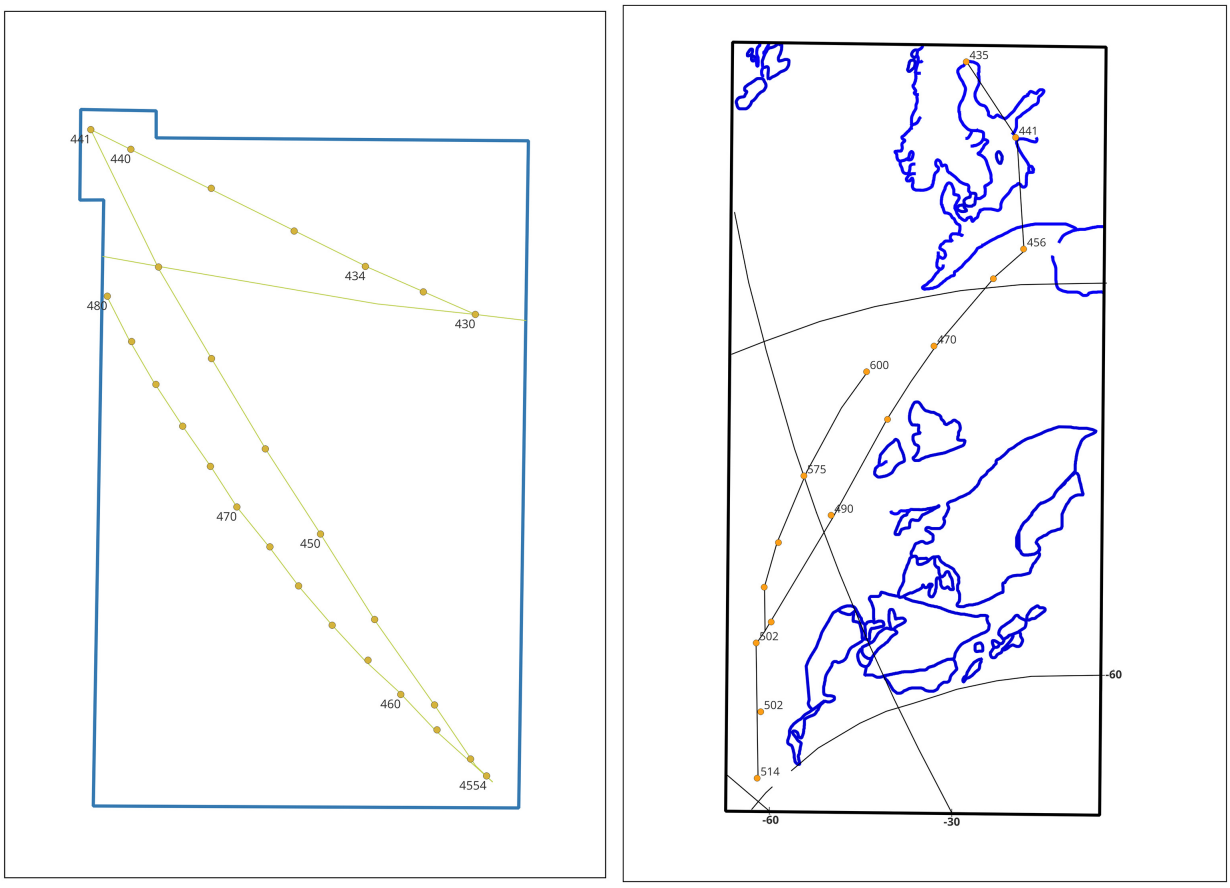

(A) (B)

Figure 16. Change of plate motion for Hawaii (A): 455.4 Ma = Sandbian, 441 Ma = Rhuddanian/Aeronian b., and for Fennoscandia (B): 441 Ma.

4.1. Clay Mineralogy: Pelite-Tuffite Assemblage

The grey-green oxygen-deficient pelite/tuffite intercalations appear after the Hiswah-MFS synchronously with the Lockne impact, Sweden [8], and the beginning of global subduction-related explosive tephra volcanism up to the top of the Katian F. [7]. The Sandbian of Oslo exposes 33 K-bentonite layers transformed to montmorillonite and its mixed-layer minerals, encountered through the L. Ordovician; andesitic glass tuff represents the source material that underwent halmyrolysis [38]. The vari-colored 10 - 15 m thick pelite marker at the Sandian/Katian b. in S Jordan still lacks XRD-analysis, chemical, and microscopic data to reconfirm a rendezvous with the Oslo section.

The 90 m deep submarine Hirnantian graben structures of Jordan had a connection to the glaciated hinterland, as verified by faceted/striated pebbles in the lag deposits of the amalgamated FUCs, deposited as glacio-fluvial sediments transported via meltwater.

4.2. Climate Forcing

According to the definition of positive/negative climate forcing (Watt/m^2) [39] (**Figure 17**), the volatile/tephra ratio, Eh, pH, and lithofacies are useful tools for understanding climate variation in fossil-free sequences [40]. Thus, the quartz arenitic FUCs of the Upper Cambrian to Lower Ordovician relate to environmental acidification caused by degassing during Wadi Araba rifting under tropical positive climate forcing (volatiles/tephra > 1, pH < 7). In contrast, after the MAB (~470 Ma), global tephra eruption led to manifold changes in lithofacies/mineralogic composition, such as arkosic siliciclastic tempestite (CUCs), oxygen-deficient pelite/tuffite cycles, and black-shale facies during the Sandbian to Katian. They reflect negative climate forcing during increasing cloudiness, temperature fall, and the onset of glaciation in the Gondwana hinterland [21] ("cosmic winter").

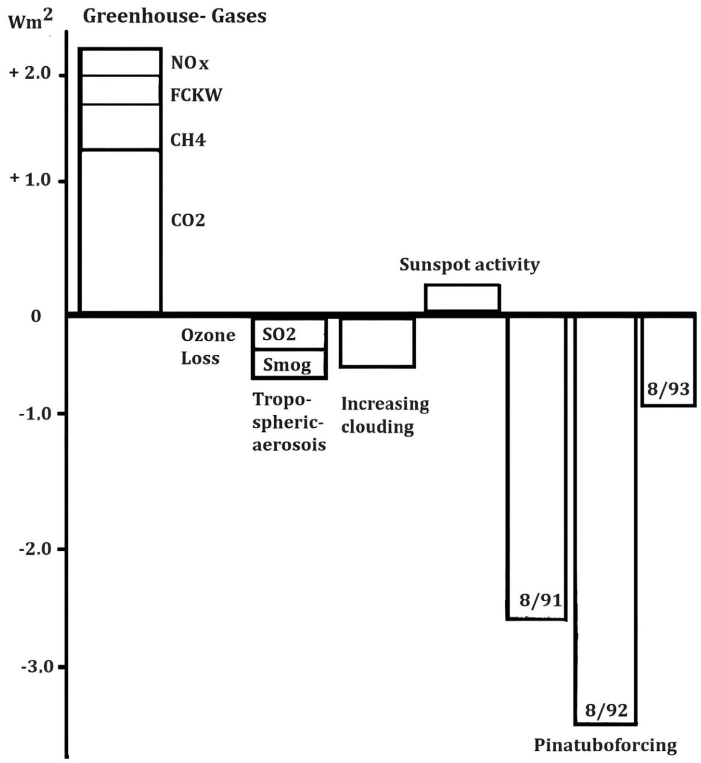

Figure 17. Positive and negative climate forcing in Watt/m^2, [39].

During the Hirnantian transtensional tectonics, the marine "canyons" hosted turbiditic FUCs overlain by a continuous transition of shallow marine and black-shale facies, intercalated with tempestites during tephra eruption in the Carnian Alps [7]. Irregularly distributed black-shale facies were deposited outside "canyons" [22] [28] [29] (**Figures 12-14**).

4.3. Volcanism Directs Isotope Data [21] (Figure 15)

Tephra eruptions and the volatile/tephra ratio play a major role in interpreting

δ^{13}C-, δ^{18}O and δ^{87}Sr/^{86}Sr-data: Negative δ^{13}C- (−1‰) and low δ^{18}O- (−10‰) excursions characterize the Tremadocian during Wadi Araba rifting/degassing, followed by an increase through the Floian until the MAB-event (~470 Ma). Since the Floian/Dapingian b., massive tephra production worked with undulations throughout the M./U. Ordovician, yielding a uniform δ^{13}C-base level (~0‰), while a first δ^{18}O-maximum (−6‰) marks the Dapinguan/Darriwilian b. During the mid-Darriwilian, MFS O 30 (469 Ma) culminates in black-shale facies exhibiting, synchronously with the Lockne impact [8], a positive δ^{13}C-excursion (+2‰) and the beginning of tuffitic pelite/tempestite-cycles during the continuous rise of δ^{18}O.

Through the Sandbian, δ^{13}C varies ~ 0‰ and shows a second positive excursion (G/CE: +2.3‰) at the Sandbian/Katian b. immediately after the second ^{18}O maximum (−5‰). This was the time-span when the most intensive tephra fall, a significant descent of δ^{87}Sr/^{86}Sr, and synsedimentary transtensional channeling took place.

Throughout the Katian, the tuffitic pelite/tempestite cycles cause the undulation of δ^{13}C ~0‰, including two positive excursions up to −2‰, as well as a steady δ^{18}O rise, while the ^{87}5sr/^{86}Sr ratio remains stable.

The L. Hirnantian (446 - 445 Ma) exhibits a high positive δ^{13}C-excursion (+7‰) coinciding with the synsedimentary transtensional submarine canyon-rifting (FUC-deposition!), accompanied by a third δ^{18}O-maximum to be interpreted as a short and strong methane eruption!

4.4. Photosynthesis and Black-Shale Facies [41] [42] (Figure 17, Figure 18)

While intensive tephra production contributes to negative climate forcing, a decrease of temperature and solar radiation --> "cosmic winter" → regional glaciation), CO_2-degassing causes ocean water acidification and becomes a fertilizer during assimilation: 6 CO_2 + 6 H_2O + 675 kcal --> $C_6H_{12}O_6$ + 6 O_2. Thereby, ~2% of CO_2 contributes to photosynthesis and 98% undergoes evaporation as heat energy. Further, from a solar radiation of >20000 Lux, the increase of assimilation ceases, and CO_2-assimilation works only between 0˚C - 30˚C [42].

The linear assimilation increases with increasing CO_2-concentration as fertilizer by causing higher phytoplankton production (Dasycladacea); however, pCO_2 >1200 ppm provides a growing CO_2/O_2-ratio, final overproduction, and consequent decay of phytoplankton for the formation of black-shale facies (**Figure 18**). Because of δ^{18}O-enrichment in seawater, its positive excursion increases phytoplankton production; its decrease, however, originates decay and fall of Eh. Further, nitrobacteria support an additional pH-decrease by chemosynthesis [43]:

$$2\ NH_3 + O_2 \text{ --> } 2\ HNO_2 + H_2O + 158\ kcal$$

$$2\ HNO_2 + O_2 \text{ --> } 2\ HNO_3 + 43.2\ kcal.$$

The reason for the positive δ^{13}C excursion lies in the preferred fixation of ^{12}C in

phytoplankton during volcanic CO_2 production when the O_2 deficit initiates decay by decreasing assimilation.

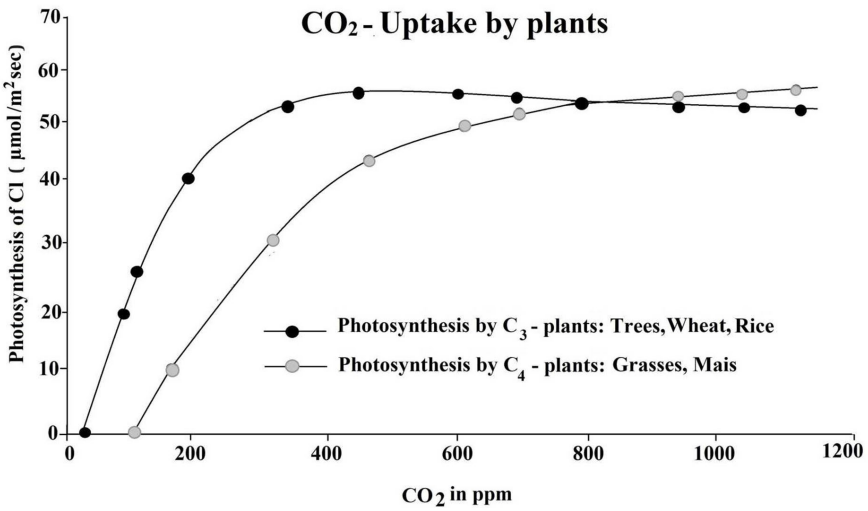

Figure 18. Photosynthesis ends at ~55 µmol/m²·sec. and 1200 ppm > CO_2. Additional CO_2-degassing increases the CO_2/O_2 ratio and lowers pH; consequently, black-shale conditions arise [41].

The total organic content (TOC) of the Ordovician/Silurian b, Mudawwara area black shale ranges from 2% to 8% [29].

4.5. Eh/pH-Interplay

The almost carbonate-free Ordovician sequence of S Jordan contains a low number of species and individuals, except in a few arkosic sandstone beds of the L. Ordovician (**Figure 4**). Environmental acidification caused by volcanic/impact? degassing led to pH 7 on land and pH ~7 - 8.4 in sea water (comp. [40]). Accordingly, body fossil assemblages merely comprise chitin- and phosphate-bearing skeletons like graptolite sp., lingulacean brachiopods, and acritarchs.

The Cruziana ichnofacies indicates periods of moderate sea level rise [34] for increasing pH during volcanic passivity, while Skolithos-endobenthos mirrors unfavorable conditions during tuffite deposition. Only the L./M. Cambrian Burj F. bears fully marine conditions with calcitic skeletons (brachiopods).

4.6. Earth's Feedback System [35]

According to Brink [35], global geodynamic cycles reveal a feedback system of the Earth throughout the Phanerozoic:

- High global sea level (HST) and the maximum of magmatic activity along the Pacific margin represent a global feature and occur almost synchronously (**Figure 19(A)**).
- Tidal dissemination occurs during normal magnetization; however, it is delayed after magmatic activity (**Figure 19(B)**).

— Decrease of the Moon's recession rate (~500 - 440 Ma) coincides with increasing magmatic activity and sea level rise (Figure 19(C)).

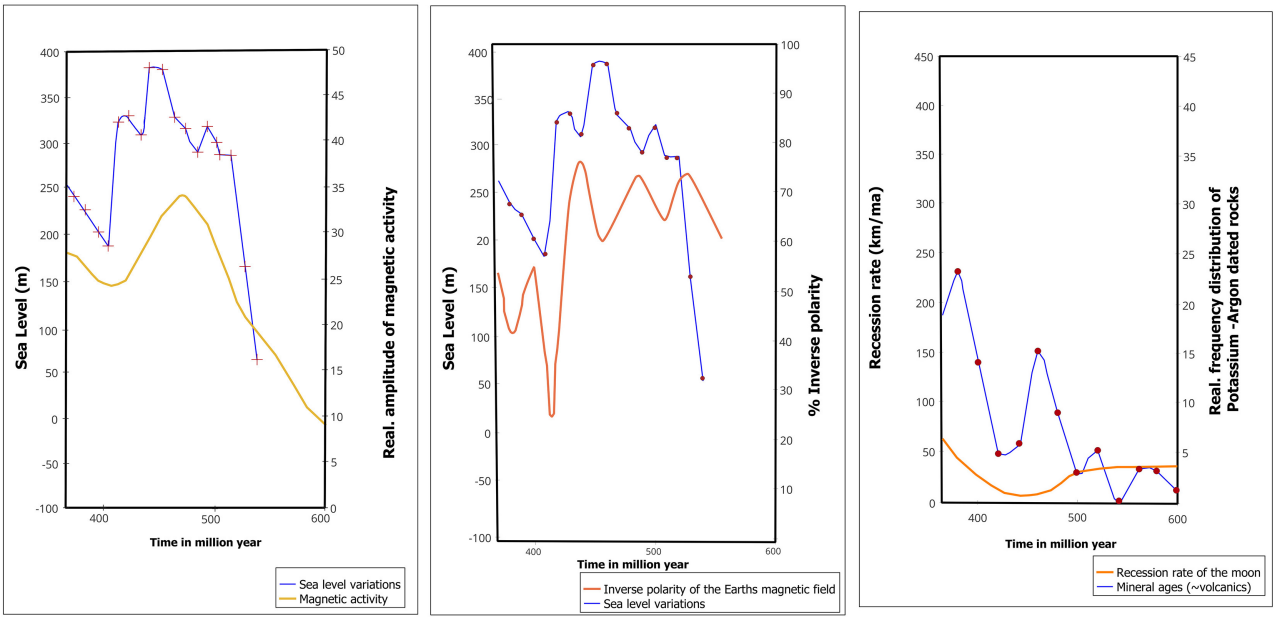

(A) (B) (C)

Figure 19. Interdependence/dependence of geodynamic cycles on Earth with the change in Moon recession rate [35]. A: A maximum of tephra production [7] correlates with a global maximum of volcanic activity and a lower Moon recession rate during the Upper Sandbian [35]; B: Negative correlation of sea level with the inverse polarity of the Earth's magnetic field; C: Delay of sea-level rise after the maximum of global Sandbian magmatic activity and the beginning of tephra production and the MAB-event (~470 Ma).

4.7. Applied to the Ordovician of S Jordan

— Low tidal dissemination (LST) and high siliciclastic input coincide with low magmatic activity, low δ^{13}C- and δ^{18}O-values during normal magnetization (U. Cambrian-L. Ordovician).

— Increasing tidal dissemination (TST → MFS) follows the MAB-event synchronously with the Moon's recession rate change, the onset of impacting, subduction-related tephra production, and a significant drop of the $\delta^{87}Sr/^{86}Sr$ ratio (M. Ordovician).

— Maximal tidal dissemination (HST) coincides with a high number of tempestite/; tuffitic pelite-cycles across the Upper/Lower shore-face.

— Through the Hirnantian, transtensional tectonics and massive tephra production correlate with positive δ^{13}C- and δ^{18}0-excursions, as evidenced by hollowed sea bottoms and black-shale facies inside and outside of the marine graben structures ("canyons").

4.8. Cyclicity [3] [18]-[20]

On the Arabian Shelf, the MFSs O20, O30, and O40 (Figure 3) occur at intervals of 14 Ma, 15 Ma, and 13 Ma, while MFS O10 represents on the Jordanian Platform

an uncertain unconformity (SB: 502 Ma) and an extreme increase of siliciclastic input (Disi F.). MFS O40 meets the Sandbian/Kation b. [7] [43]: 452,621 ± 0.39 Ma) and the Hawaian plate motion change [44] [45] that happened after the Lockne/Malungen impact [8].

After the MAB-event (470 - 444 Ma), the eight minor impacts took pace over time spans of 1 - 6 Ma.

The Sandbian and Katian sedimentary cycles of Jordan [22] [28] [29] exposing ichnofacies, tempestite-cycles, and δ^{13}C-data relate to the subduction-related explosive volcanic arc tephra eruptions, the 33 K-bentonite-intercalations (Arnstad F.) at the Sinsen/Oslo location (**Figure 7**), while the late Hirnantian tephra eruptions of the Carnian Alps finally became most relevant as driving forces for the abiotic/biotic revolution throughout the M.-U. Ordovician and the Hirnantian-Rhuddanian b.

4.9. Ordovician-Silurian Boundary or Transitional Zone?

According to GSSP [10], the Ordovician-Silurian b. (444 Ma) is biostratigraphically defined by Akidograptus ascensus, appearing at the Rhuddanian base.

In the type area of the Batn en Ghul Mudawwara region, the lower Member of the black-shale bearing Batra F. was deposited inside the graben structure and still belongs to the uppermost Hirnantian, while its middle Member covers the 0-S b. transitional zone, and its upper M. the U. Rhuddanian [28] [29]; all together contain a broad graptolite spectrum.

Figure 14(C) shows the transtensional pull-apart structure at Jebel Ammar and Jebel Umeir, which exhibits a continuous sequence of conformably bedded proximal turbidites (FUCs), silty/sandy mass flows, shore-face brachiopod-bearing arkosic clastics overlain with thin-bedded black shale and tempestites (Hcs) of the L. Batra M. [25] [26] [28] [29].

As directed by transtensional tectonics, and possibly deposited below a halocline [29], this transition zone seems to be a regional phenomenon without MFS-character of the black-shale facies; it rather hints at a strong methane eruption during pull-apart tectonics (see isotope data (**Figure 15**)). Outside the "canyons," there seems to be no indication of any unconformity through the shallow marine siliciclastic Batra F., which is overlain by the sandy Ratiya F. [25] (**Figure 14(A)**).

The L. Silurian of the Saudi Arabia/Oman shelf areas is dominated by an "amalgamated" MFS S 10 [3]: (~441/440 Ma), which represents, as a black-shale facies, the most important Early Paleozoic hydrocarbon source interval in the Near/Middle East (**Figure 3**).

Finally summarized, the major driver for black-shale facies formation was sourced in the Sandbian-Katian subduction-related explosive tephra-volcanism. It acted as a global spreader and fertilizer for phytoplankton production, which led to overproduction, negative climate forcing, and decay of organic matter. Global volcanism ceased during the Silurian except in N America (Appalachian).

5. Closing Statement

"Gaia is merely a useful name for a worldwide phenomenon: the regulation of temperature, acid-base equilibrium, and gas composition. Gaia is the total of interagitating ecosystems that form a unique, powerful ecosystem on Earth."

"Gaia is in her complete symbiogenetic magnificence by her being: expansive, cunning, aesthetic, very ancient, and extremely resistant."

Lynn Margulis, Biologist [46]

Acknowledgements

We gratefully appreciate the digital support of O. Schneider and K. Paris.

Conflicts of Interest

The authors declare no conflicts of interest regarding the publication of this paper.

References

[1] Husseini, M.I. (1989) Tectonic and Deposition Model of Late Precambrian-Cambrian Arabian and Adjoining Plates. *AAPG Bulletin*, **73**, 1117-1131. https://doi.org/10.1306/44b4a54b-170a-11d7-8645000102c1865d

[2] Geert, K., Afifi, A.M., Al-Hajri, S.A. and Droste, H.J. (2001) Paleozoic Stratigraphy and Hydrocarbon Habitat of the Arabian Plate. *GeoArabia*, **6**, 407-442. https://doi.org/10.2113/geoarabia0603407

[3] Haq, B.U. and Al-Qahtani, A.M. (2005) Phanerozoic Cycles of Sea-Level Change on the Arabian Platform. *GeoArabia*, **10**, 127-160. https://doi.org/10.2113/geoarabia1002127

[4] Caputo, M.V. and Crowell, J.C. (1985) Migration of Glacial Centers across Gondwana during Paleozoic Era. *Geological Society of America Bulletin*, **96**, 1020-1036. https://doi.org/10.1130/0016-7606(1985)96<1020:mogcag>2.0.co;2

[5] Vaslet, D. (1990) Upper Ordovician glacial deposits in Saudi Arabia. *Episodes*, **13**, 147-161. https://doi.org/10.18814/epiiugs/1990/v13i3/002

[6] Abed, A.M., Makhlouf, I.M., Amireh, B.S. and Khalil, B. (1993) Upper Ordovician Glacial Deposits in Southern Jordan. *Episodes*, **16**, 316-328. https://doi.org/10.18814/epiiugs/1993/v16i1.2/003

[7] Ballo, E.G., Augland, L.E., Hammer, Ø. and Svensen, H.H. (2019) A New Age Model for the Ordovician (Sandbian) K-Bentonites in Oslo, Norway. *Palaeogeography, Palaeoclimatology, Palaeoecology*, **520**, 203-213. https://doi.org/10.1016/j.palaeo.2019.01.016

[8] Ormö, J., Sturkell, E., Alwmark, C. and Melosh, J. (2014) First Known Terrestrial Impact of a Binary Asteroid from a Main Belt Breakup Event. *Scientific Reports*, **4**, Article No. 6724. https://doi.org/10.1038/srep06724

[9] Sheehan, P.M. (2001) The Late Ordovician Mass Extinction. *Annual Review of Earth and Planetary Sciences*, **29**, 331-364. https://doi.org/10.1146/annurev.earth.29.1.331

[10] Stratigraphic Chart of Germany Compact, GSSP (2017) Potsdam (GFZ).

[11] Al-Husseini, M.I. (2000) Origin of the Arabian Plate Structures: Amar Collision and Najd Rift. *GeoArabia*, **5**, 527-542. https://doi.org/10.2113/geoarabia0504527

[12] Jarrar, G.H. (1985) Late Proterozoic Crustal Evolution of the Arabian Nubian Shield

in the Wadi Araba, SW Jordan. Bundesanstalt für Geowissenschaften und Rohstoffe, 3-87.

[13] Jarrar, G., Wachendorf, H. and Zellmer, H. (1991) The Saramuj Conglomerate: Evolution of a Pan-African Molasse Sequence from Southwest Jordan. *Neues Jahrbuch für Geologie und Paläontologie—Monatshefte*, **1991**, 335-356. https://doi.org/10.1127/njgpm/1991/1991/335

[14] Jarrar, G., Wachendorf, H. and Saffarini, G. (1992) A late Proterozoic bimodal volcanic/Subvolcanic suite from Wadi Araba, southwest Jordan. *Precambrian Research*, **56**, 51-72. https://doi.org/10.1016/0301-9268(92)90083-z

[15] Jarrar, G., Wachendorf, H. and Zachmann, D. (1993) A Pan-African Alkaline Pluton Intruding the Saramuj Conglomerate, South-West Jordan. *Geologische Rundschau*, **82**, 121-135. https://doi.org/10.1007/bf00563275

[16] Amireh, B.S., Schneider, W. and Abed, A.M. (1994) Evolving Fluvial—Transitional—Marine Deposition through the Cambrian Sequence of Jordan. *Sedimentary Geology*, **89**, 65-90. https://doi.org/10.1016/0037-0738(94)90084-1

[17] Vail, P.R., Mitchum Jr., R.M. and Thompson, S. (1977) Seismic Stratigraphy and Global Changes in Sea Level. Part 4: Global Cycles of Relative Changes of Sea Level. In: Payton, C.E., Ed., *Seismic Stratigraphy—Applications to Hydrocarbon Exploration*, American Association of Petroleum Geologists, 83-97.

[18] Schneider, W., Amireh, B.S. and Abed, A.M. (2007) Sequence Analysis of the Early Paleozoic Sedimentary Systems of Jordan. *Zeitschrift der Deutschen Gesellschaft für Geowissenschaften*, **158**, 225-247. https://doi.org/10.1127/1860-1804/2007/0158-0225

[19] Schneider, W. and Salameh, E. (2012) Did Major Impacts Affect Sedimentologic/sequence-Analytical Pattern of the Early Palaeozoic Sedimentary Systems of Jordan, Arabian Plate? *Open Journal of Geology*, **2**, 241-252. https://doi.org/10.4236/ojg.2012.24024

[20] Amireh, B.S., Schneider, W. and Abed, A.M. (2001) Fluvial-Shallow Marine-Glaciofluvial Depositional Environments of the Ordovician System in Jordan. *Journal of Asian Earth Sciences*, **19**, 45-60. https://doi.org/10.1016/s1367-9120(00)00010-9

[21] Clube, V. and Napier, B. (1990) The Cosmic Winter. Blackwell.

[22] Miall, D. (1996) The Geology of Fluvial Deposits. Springer, 582 p.

[23] Schneider, W. and Salameh, E. (2020) Phanerozoic Quartz Arenite Formation and Sequence-Analytical Patterns: Indirectly Relating to Major Impacting and Super Plume Volcanism, Jordan, Arabian Plate. *Open Journal of Geology*, **10**, 13-52. https://doi.org/10.4236/ojg.2020.101002

[24] Amireh, R.S. (1987) Sedimentologic and Petrologic Interplays of the Nubian Series in Jordan with Regard to Paleogeography and Diagenesis. Ph.D. Thesis, Braunschweig University, 232 p.

[25] Makhlouf, I.M. (1995) Tempestite Facies Diplaying Hummocky Cross-Stratification and Subaqueous Channels in Ordovician Shelf Deposits, S Jordan. *Africa Geoscience Review*, **2**, 91-99.

[26] Amireh, B.S., Schneider, W. and Abed, A.M. (1994) Diagenesis and Burial History of the Cambrian-Cretaceous Sandstone Series in Jordan. *Neues Jahrbuch für Geologie und Paläontologie—Abhandlungen*, **192**, 151-181. https://doi.org/10.1127/njgpa/192/1994/151

[27] Powell, J.H., Moh'd, B.K. and Masri, A. (1994) Late Ordovician—Early Silurian Glaciofluvial Deposits Preserved in Palaeovalleys in South Jordan. *Sedimentary Geology*,

89, 303-314. https://doi.org/10.1016/0037-0738(94)90099-x

[28] Armstrong, H.A., Turner, B.R., Makhlouf, I.M., Weedon, G.P., Williams, M., Al Smadi, A., *et al.* (2005) Origin, Sequence Stratigraphy and Depositional Environment of an Upper Ordovician (Hirnantian) Deglacial Black Shale, Jordan. *Palaeogeography, Palaeoclimatology, Palaeoecology*, **220**, 273-289. https://doi.org/10.1016/j.palaeo.2005.01.007

[29] Andrews, I.J. (1991) Paleozoic Lithostratigraphy in the Subsurface of Jordan. *Subsurface Geology: Bull*, **2**, 75 p.

[30] Sharland, P.R., Casey, D.M., Davies, R.B., Simmons, M.D. and Sutcliffe, O.E. (2004) Arabian Plate Sequence Stratigraphy—Revisions to SP2. *GeoArabia*, **9**, 199-214. https://doi.org/10.2113/geoarabia0901199

[31] Burgarth, K.P., Hagen, D. and Sievers, U. (1984) Geochemistry, Geology and Primary Copper Mineralization in Wadi Araba, Jordan. Geologisches Jahrbuch Reihe B, **53**, 3-53.

[32] Augland, L.E., Ryabov, V.V., Vernikovsky, V.A., Planke, S., Polozov, A.G., Callegaro, S., *et al.* (2019) The Main Pulse of the Siberian Traps Expanded in Size and Composition. *Scientific Reports*, **9**, Article No. 18723. https://doi.org/10.1038/s41598-019-54023-2

[33] Svensen, H., Planke, S., Polozov, A.G., Schmidbauer, N., Corfu, F., Podladchikov, Y.Y., *et al.* (2009) Siberian Gas Venting and the End-Permian Environmental Crisis. *Earth and Planetary Science Letters*, **277**, 490-500. https://doi.org/10.1016/j.epsl.2008.11.015

[34] Svensen, H.H., Jerram, D.A., Polozov, A.G., Planke, S., Neal, C.R., Augland, L.E., *et al.* (2019) Thinking about Lips: A Brief History of Ideas in Large Igneous Province Research. *Tectonophysics*, **760**, 229-251. https://doi.org/10.1016/j.tecto.2018.12.008

[35] Seilacher, A. (1992) An Updated Cruziana Stratigraphy of Gondwana Paleozoic Sandstones, In: Sahlem, M.S., Ed., *The Geology of Libya*, *Part* 8, Elsevier, 1565-1581.

[36] Brink, H. (2006) Do the Global Geodynamic Cycles of the Phanerozoic Represent a Feedback System of the Earth and Is the Moon Involved as an Acting External Force? *Zeitschrift der Deutschen Gesellschaft für Geowissenschaften*, **157**, 17-40. https://doi.org/10.1127/1860-1804/2006/0157-0017

[37] Villas, E. and Cocks, L.R.M. (1996) The First Early Silurian Brachiopod Fauna from the Iberian Peninsula. *Journal of Paleontology*, **70**, 571-588. https://doi.org/10.1017/s0022336000023544

[38] Harms, J.C. (1979) Primary Sedimentary Structures. *Annual Review of Earth and Planetary Sciences*, **7**, 227-248. https://doi.org/10.1146/annurev.ea.07.050179.001303

[39] Millot, G. (1970) Geology of Clays. Springer, 429 p.

[40] Schmincke, H.U. (2000) Vulkanismus. Wissensch. Buchgesellsch, 264 p.

[41] Munnecke, A., Calner, M., Harper, D.A.T. and Servais, T. (2010) Ordovician and Silurian Sea-Water Chemistry, Sea Level, and Climate: A Synopsis. *Palaeogeography, Palaeoclimatology, Palaeoecology*, **296**, 389-413. https://doi.org/10.1016/j.palaeo.2010.08.001

[42] Vahrenholt, F. and Lüning, S. (2021) Unerwünschte Wahrheiten. 6th Editon, TLMV, 352 p.

[43] Koch, H. and Siedentop, W. (1957) Grundzüge der Allgemeinen Biologie. Quelle und Neyer, 175 p.

[44] Schneider, W. and Salameh, E. (2024) Cretaceous Large Igneous Provinces (Lips) Af-

fect Sedimentary Processing: Jordan, Arabian Plate; NW Germany, Central Europe. *Open Journal of Geology*, **14**, 671-704. https://doi.org/10.4236/ojg.2024.146029

[45] Price, N.J. (2001) Major Impacts and Plate Tectonics. Routledge, 354 p.

[46] Margulis, L. (2020) Der Symbiotische Planet. Westend Verlag GmbH, 188 p.